

This is the accepted manuscript made available via CHORUS. The article has been published as:

Rapidly fluctuating orbital occupancy above the orbital ordering transition in spin-gap compounds

B. Rivas-Murias, H. D. Zhou, J. Rivas, and F. Rivadulla

Phys. Rev. B **83**, 165131 — Published 29 April 2011

DOI: [10.1103/PhysRevB.83.165131](https://doi.org/10.1103/PhysRevB.83.165131)

Rapidly fluctuating orbital occupancy above the orbital ordering transition in spin-gap compounds

B. Rivas-Murias,^{1,2} H. D. Zhou,³ J. Rivas,⁴ F. Rivadulla^{1,2,*}

¹Department of Physical Chemistry and ²Center for Research in Biological Chemistry and Molecular Materials, University of Santiago de Compostela, 15782 Santiago de Compostela, Spain

³National High Magnetic Field Laboratory, Florida State University, Tallahassee, FL 32306-4005, USA

⁴Department of Applied Physics, University of Santiago de Compostela, 15782 Santiago de Compostela, Spain

e-mail: f.rivadulla@usc.es

Several spin systems with low dimensionality develop a spin-dimer phase within a molecular orbital below T_S , competing with long-range antiferromagnetic order. Very often, preferential orbital occupancy and ordering are the actual driving force for dimerization, as in the so-called orbitally-driven spin-Peierls compounds (MgTi_2O_4 , CuIr_2S_4 , $\text{La}_4\text{Ru}_2\text{O}_{10}$, $\text{NaTiSi}_2\text{O}_6$, etc.). Through a microscopic analysis of the thermal conductivity $\kappa(T)$ in $\text{La}_4\text{Ru}_2\text{O}_{10}$, we show that the orbital occupancy fluctuates rapidly above T_S , resulting in an orbital-liquid state. The strong orbital-lattice coupling introduces dynamic bond-length fluctuations that scatter the phonons to produce a $\kappa(T) \sim T$ (*i.e.* glass-like) above T_S . This phonon-glass to phonon-crystal transition is shown to occur in other spin-dimer systems, like $\text{NaTiSi}_2\text{O}_6$, pointing to a general phenomenon.

Preferential orbital occupation in transition-metal compounds shapes the chemical bond of these systems, and is the origin of many different long-range magnetic and charge arrangements.¹ In magnetically frustrated structures, or slightly correlated low dimensional systems with small spin ($S < 1$), long-range ordering of spin-dimers (singlets) competes with antiferromagnetic (AF) order,² as in pyroxene $\text{NaTiSi}_2\text{O}_6$ ($S = 1/2$)³. In layered $\text{La}_4\text{Ru}_2\text{O}_{10}$ ($S = 1$), Wu *et al.*⁴ proposed that an orbital ordering: $[\text{dxz}^{\uparrow\downarrow}, \text{dxy}^{\uparrow}, \text{dyz}^{\uparrow}]$ introduces a strong exchange anisotropy that drives the system electronically 1D, and forms $\text{Ru}^{4+}\text{-Ru}^{4+}$ spin-singlets below $T_S \approx 160$ K (a realization of an orbitally driven Peierls state).⁵ This anisotropy is reflected in alternating short/long Ru-O bond-lengths in the low temperature (spin-gapped) phase (see Figure 1). However, these bond-distances are also compatible with an $S = 0$ at each Ru^{4+} site ($\text{dxz}^{\uparrow\downarrow}, \text{dxy}^{\uparrow\downarrow}, \text{dyz}^0$), as originally proposed by Khalifah *et al.*⁶; and to distinguish between these scenarios is a difficult task.⁷

At high temperature, $T > T_S$, the undistorted Ru-O octahedra observed by neutron diffraction have been assigned to an equal orbital occupation that quenches the orbital degrees of freedom. But these equal bond-lengths could also be a consequence of a rapid fluctuation in the orbital occupancy, which does not quench the orbital channel but results in an average Ru-O bond. This subtle difference between equal vs. rapidly fluctuating orbital occupancy is really important, as it should change the way we describe the

bond in solids above a static long-range orbital-order transition. For example, fluctuations in the orbital occupancy should manifest as variations in the bond-length that must influence the propagation of phonons, and according to the Goodenough-Kanamori rules¹ should introduce a rapid fluctuation in the sign of the magnetic exchange.

Here we report the analysis of thermal conductivity in $\text{La}_4\text{Ru}_2\text{O}_{10}$ and $\text{NaTiSi}_2\text{O}_6$, and show that their high-temperature phase above T_S is better described by a mixture or a resonance between different structures determined by rapid fluctuating orbital occupancies, instead of an average occupancy that quenches the orbital degrees of freedom. This effect leads to a dramatic change in the temperature dependence of $\kappa(T)$, that shows a phonon-crystal to phonon-glass transition at T_S .

Polycrystalline samples of $\text{La}_4\text{Ru}_2\text{O}_{10}$ (and Ce-doped $\text{La}_{4-x}\text{Ce}_x\text{Ru}_2\text{O}_{10}$) and $\text{NaTiSi}_2\text{O}_6$, were synthesized by solid state reaction. For $\text{La}_4\text{Ru}_2\text{O}_{10}$, stoichiometric amounts of La_2O_3 and RuO_2 (pre-dried at 900°C and 600°C overnight, respectively) were grounded and annealed at 1150°C for 24h in air, with an intermediate ground. In order to obtain dense pellets for thermal conductivity measurements, the powders were cold-pressed in a tungsten carbide anvil at ~ 0.3 GPa before the last annealing. The Seebeck coefficient was monitored to ensure a correct oxygen stoichiometry.

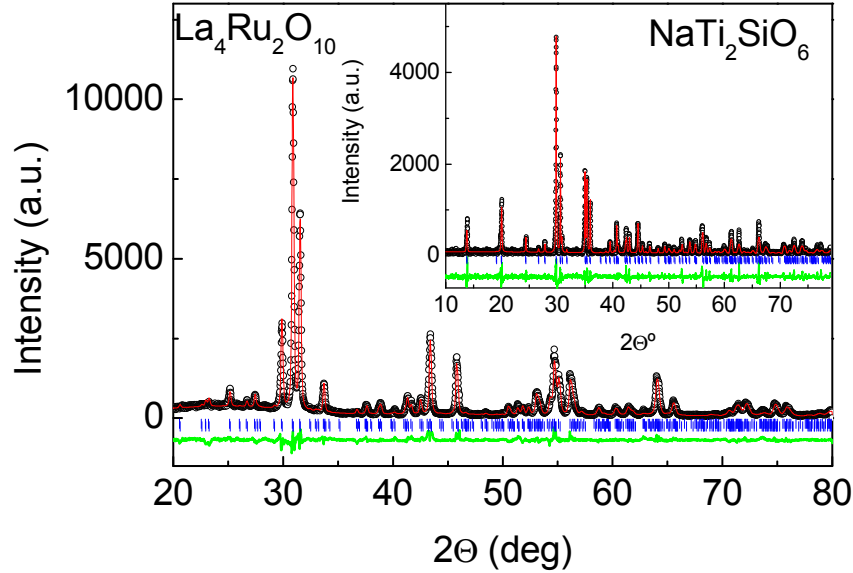


Figure 1. Refinement of the x-ray powder patterns of $\text{La}_4\text{Ru}_2\text{O}_{10}$ (main panel) and $\text{NaTi}_2\text{SiO}_6$ (inset). Open symbols, and solid line represent the observed and calculated diffraction patterns, respectively. The horizontal line represents the difference between both curves, and the vertical bars are the position of the allowed reflections for each symmetry space group.

For $\text{NaTi}_2\text{SiO}_6$, a precursor of $\text{Na}_2\text{TiSi}_4\text{O}_{11}$ was first prepared by solid state reaction of the appropriate mixture of Na_2CO_3 , TiO_2 , and SiO_2 at 800 °C in air for 15 hours. $\text{NaTi}_2\text{SiO}_6$ was prepared by reacting a

mixture of $\text{Na}_2\text{TiSi}_4\text{O}_{11}$, Ti, and TiO_2 at 1170°C in Ar for one day. Rietveld refinement of x-ray powder patterns showed the structure and lattice parameters in agreement with the literature, for both compounds (Figure 1).

Thermal conductivity, $\kappa(T)$ was measured by the steady-state method in a home-made setup, under vacuum ($\approx 10^{-5}$ mbar). Different gradients (between 0.5K and 5K) were established between two points of the sample, and $\kappa(T)$ was obtained from the linear fit of the data. The error of the measurement (mainly from the dimensions of the sample and heat losses) is estimated $\approx 10\%$, by comparison with standardized samples with similar thermal conductivity. Radiation losses were considered, but are negligible at the temperatures studied in this paper.

The crystal structure of $\text{La}_4\text{Ru}_2\text{O}_{10}$ can be described as zigzag chains of corner sharing RuO_6 along b axes in the ab plane (see Figure 2).⁶ The high-temperature (HT) monoclinic phase is characterized by equal Ru-Ru distances; in the low-temperature (LT) triclinic phase there is a lengthening (shortening) of the bond distance along the x (y) direction (Figure 1).⁶ The orbital manifold of low spin Ru^{4+} ($4d^4$) splits in an octahedral environment into a lower energy $xz^{\uparrow\downarrow}$ and a degenerate $xy^{\uparrow} yz^{\uparrow}$. An ab-initio calculation proposed that the energy difference between the doubly occupied orbital and the single occupied doublet increases from ≈ 50 meV in the HT phase to ≈ 300 meV in the LT phase.⁴ The strong exchange anisotropy induced by the orbital ordering forms a Ru-Ru molecular-orbital along the short bonds, opening a spin gap in the low-temperature phase.⁴ On the basis of this interpretation $\text{La}_4\text{Ru}_2\text{O}_{10}$ has been proposed as a rare example of a spin-dimer system with $S > 1/2$ and 2D structure, due to an unusually strong orbital anisotropy in a 4d system. Optical conductivity data by Moon *et al.*⁸ support this interpretation, over the initial proposal of $xy^{\uparrow\downarrow} yz^{\uparrow\downarrow}$ ($S=0$ at Ru^{4+} sites) in Ref. [6].

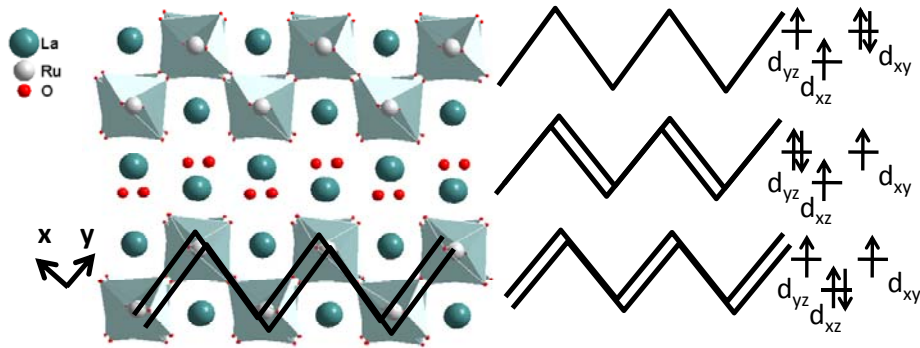


Figure 2. Left: Crystal structure of $\text{La}_4\text{Ru}_2\text{O}_{10}$ (ab plane viewed along the c direction). The solid lines show the short (double) and long (single) bonds in the low temperature monoclinic phase. There is another single bond along the c -axis (not shown). Right: Spin-orbital configurations of the t_{2g} orbital set in Ru^{4+} , along with the resulting bond-configuration in the xy plane. Double (single) bonds represent short (long) Ru-O-Ru bonds. The actual energy difference between the different orbital sets is not represented. For the orbital configuration on the top there is another short bond along the c -direction (not shown).

In Figure 3, we show the temperature dependence of the magnetic susceptibility for $\text{La}_4\text{Ru}_2\text{O}_{10}$ at different pressures. The transition temperature increases with pressure at a rate $\partial \ln T_s / \partial P = 3.83 \times 10^{-2} \text{ GPa}^{-1}$. This increase with pressure is consistent with an interionic exchange coupling of the form $J \sim t^2/U$, hence supporting the formation of spin dimers instead of the $\text{Ru}^{4+} S=0$ state. Also, although we did not measure experimentally the bulk modulus, B , for $\text{La}_4\text{Ru}_2\text{O}_{10}$, it must be similar to $\text{Ba}_4\text{Ru}_3\text{O}_{10}$ ($B=113 \text{ GPa}^{-1}$),⁹ given their similar coordination. Assuming this value, the Bloch's parameter¹⁰ $\alpha = \partial \ln T_s / \partial V \approx 4.2$. The calculated α for AF insulators with direct $d-d$ overlap is 3.3, and 4.6 for a $d-p-d$ transfer.¹¹ This volume dependence of the susceptibility shows that the most probable path for the exchange interaction goes through the O:2p orbitals, that is, the spin-singlet state involves the Ru-O-Ru atomic trimer.

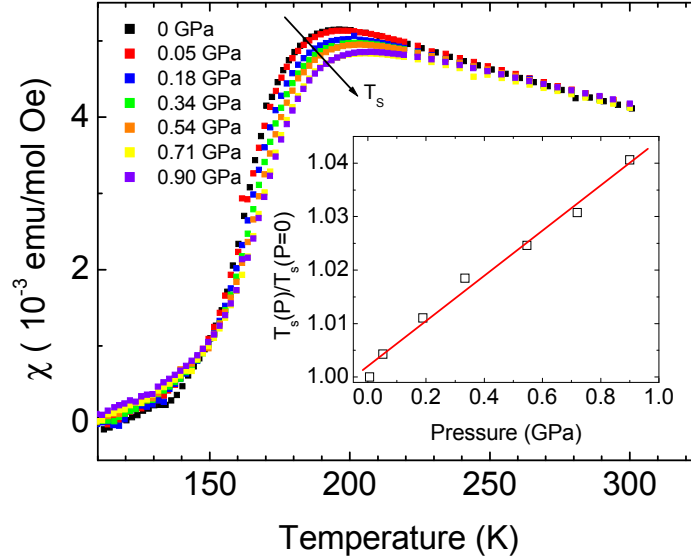


Figure 3. Temperature dependence of the magnetic susceptibility for $\text{La}_4\text{Ru}_2\text{O}_{10}$ at different pressures. Inset: Evolution of the transition temperature T_s with pressure.

On the other hand, the assumption that orbital degrees of freedom are quenched above T_s left the HT phase practically unexplored. However, with such a small energy difference $\approx 50 \text{ meV}$ between the $xz^{\uparrow\downarrow}$ and $xy^{\uparrow}yz^{\uparrow}$ states in the HT phase, fast fluctuations in the orbital occupancy are highly probable. Actually, Moon *et al.*⁸ observed a gradual development of the in-plane anisotropy above T_s , and suggested that short-range orbital or spin correlations could survive above the spin gap temperature.

Due to the anisotropy in the bond-distance induced by the orbital ordering (see Figure 2, right), a rapid fluctuation in the orbital occupancy should manifest in a fluctuation in the bond-distance, undetectable in a conventional diffraction experiment.

However, other magnitudes like thermal conductivity or the speed of sound should be sensitive to these bond-length fluctuations, if present. The temperature dependence of the thermal conductivity for $\text{La}_4\text{Ru}_2\text{O}_{10}$ is shown in Figure 4. There is a dramatic change in the mechanism of heat-conduction at the magneto-structural transition at T_s . Given the large electronic resistivity, the cause of this effect must be in a fundamental change of the lattice contribution to the thermal conductivity. The behavior of the LT-phase is typical for a crystalline material, with a phonon peak at the maximum phonon mean-free path, Λ , and the characteristic reduction of $\kappa(T > T_{\max})$ as temperature increases due to Umklapp scattering.¹² However, κ changes drastically its temperature dependence above T_s , increasing linearly with T in the HT phase as it is expected for an amorphous solid.¹² Although the absolute values of κ do not change appreciably, it is clear that spectra of low energy excitations of the lattice change completely in the HT phase with respect to the LT spin-dimerized state.

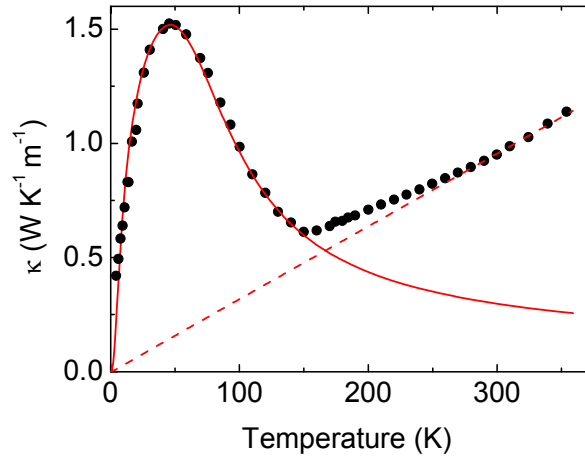


Figure 4. Temperature dependence of the thermal conductivity in $\text{La}_4\text{Ru}_2\text{O}_{10}$. Solid and dashed lines represent the fittings to equation (1) in the low and high temperature regimes, respectively, as explained in the text.

In a first approximation, the thermal conductivity can be estimated by the Debye model:¹³

$$\kappa(T) = \frac{1}{2\pi^2\nu} \int_0^{\omega_D} \tau(\omega) \frac{\hbar\omega^4}{k_B T^2} \frac{e^{\hbar\omega/k_B T}}{(e^{\hbar\omega/k_B T} - 1)^2} d\omega \quad (1)$$

where ν and ω_D are the sound velocity and the Debye frequency, respectively, and the other symbols have their usual meaning. The relaxation time, $\tau(\omega)$ is the sum of the contribution of different processes that produce an effective phonon scattering. In our analysis we have included three different terms:

$$\tau^{-1}(\omega) = A + B\omega^2 T e^{-\Theta/\omega T} + C\omega^n$$

$$A = \frac{v}{1.8d}$$

$$B = \frac{\hbar\gamma^2}{Mv^2\Theta}$$
(2)

The first term represents the scattering by grain boundaries in polycrystalline materials ($d \approx 1 \pm 0.2 \mu\text{m}$ is the grain size obtained from electron microscopy, while the average phonon velocity, v , was estimated from the Debye temperature, Θ); the second term represents the Umklapp processes¹⁴ (M and γ are the average atomic mass and the Grüneisen constant, that we assumed ≈ 2 , respectively), and the last one is due to scattering by defects on the structure. For lattice-point defects, or any other object with a typical size smaller than the phonon wavelength, this reduces to Rayleigh scattering, having $n=4$ and

$$C = \frac{V_0}{4\pi v^3} \sum_i x_i S_i^2$$
(3)

where V_0 and x_i are the volume and molar fraction of defects. S represents the contributions of the local variation of mass, bond-distance and energy due to the defects on the host lattice.¹⁵ Domain boundaries in the regular propagation of short-long-short-long Ru-O bonds in the LT triclinic structure (see Figure 1, right), will create scattering centers of $\approx 8 \text{ \AA}$ in linear dimensions, and a 5% variation in the local bond-distance with respect to the regular structure.

The fitting of experimental $\kappa(T)$ to equation (1) is shown in Figure 4 (solid line). For boundary and Umklapp scattering we used the parameters calculated from our experimental data ($A = 3.6 \times 10^9 \text{ s}^{-1}$, $B = 9.9 \times 10^{-17} \text{ s K}^{-1}$ and used $\alpha=1$ as a fitting factor), except for $\Theta \approx 225 \text{ K}$, which is $\approx 30\%$ larger than obtained directly from our specific heat, although exactly the same as obtained from $C(T)$ by Malik *et al.*¹⁶ Assuming a 4% of defects ($C = 4.2 \times 10^{-41} \text{ s}^3$) results in a remarkably good agreement between the predictions from the Debye model and the experimental data in the LT dimerized phase.

Above T_s , $\kappa(T)$ departs completely from the expected behavior for a crystalline solid. Kittel¹⁷ gave the first interpretation to this behavior, assuming a constant Λ for every phonon frequency in the glass due the geometrical disordered structure. This should be a reasonable approximation, at least for small phonon wavelengths. From an analogy with the kinetic theory of gases, the thermal conductivity of a crystalline solid can be expressed as:

$$\kappa = \frac{1}{3} C v \Lambda$$
(4)

where C is the lattice heat capacity. To obtain the lattice specific heat we have fitted the background of the experimental $C(T)$ curve to a polynomial function. The magnetic contribution that results from the subtraction of this polynomial to the total heat capacity is shown in the inset to Fig. 5. Integration of this peak gives a magnetic entropy 8.56 J/mol K , only $\approx 6\%$ smaller than the theoretical value for low spin Ru^{4+} : $R \ln(2S+1) = 9.13 \text{ J/mol K}$. This supports the validity of our estimation for the lattice heat capacity.

Therefore, from the experimental values of $\kappa(T)$ and $C(T)$, and using $v=4500 \text{ ms}^{-1}$ obtained from the experimental Θ , and the theoretical density from the Rietveld fitting of the x-ray powder patterns, we have estimated the temperature dependence of Λ shown in Figure 5. Above T_s , $\Lambda \approx 25 \text{ \AA}$, and remains

practically constant up to room temperature. This should not be taken as an accurate absolute value of Λ , but as an order of magnitude, which in this case is roughly of the size of a few Ru-O-Ru bonds. This result points to anisotropic Ru-O bond-length fluctuations as the most probably source of geometrical disorder that produces the glass-like $\kappa(T > T_S)$.

So, the orbital degeneracy is already quenched at high temperature; the transition at T_S reflects an order-disorder transition among the equivalent orbital configurations, similar to the Jahn-Teller transition in LaMnO_3 .¹⁸ Although it is normally assumed that the driving force for this transition is preferential orbital occupation, ordering of the dynamic lattice distortion below T_S will also give rise to an orbital anisotropy. Whatever the case may be, preferential orbital occupation the cause or the effect of a lattice distortion, is not relevant for the results discussed here. Only the net result of a charge density wave that melts above T_S into a phase of dynamically distorted RuO_6 octahedra persisting up to room temperature is important for determining the temperature dependence of the thermal conductivity.

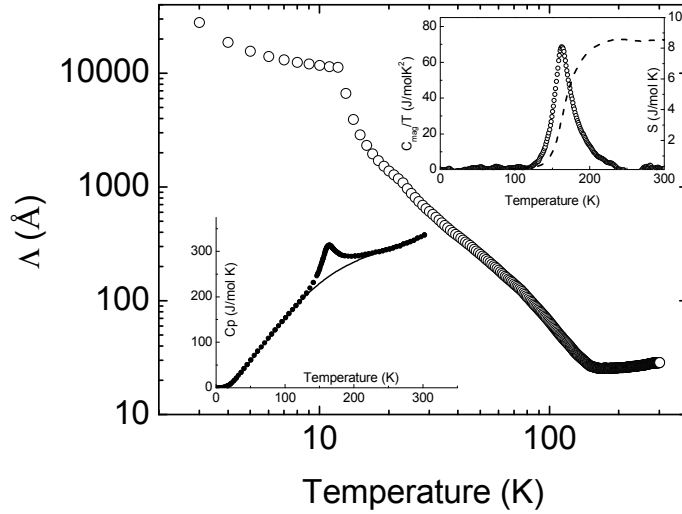


Figure 5. Temperature dependence of phonon mean free path in $\text{La}_4\text{Ru}_2\text{O}_{10}$. Lower inset: Total specific heat (circles) and estimated lattice background (line). Subtraction of the background to the total specific heat gives the magnetic contribution and the magnetic entropy (upper inset).

On the other hand, introducing 2.5% of holes into the Ru sites via Ce^{+4} -doping (Fig. 6) suppresses T_S by 15 K and $\kappa(T_{\text{max}})$ drops $\approx 50\%$. This demonstrates the relevance of cooperative lattice distortions in reducing the elastic energy and stabilizing the dimerized phase. For this reason, we think a resonance between the different bond-configurations shown in Figure 1 is more probable above T_S , than a random site-to-site fluctuation in the orbital occupancy. Therefore, resonating bonds are formed with the aid of unquenched orbital degrees of freedom, to remove the orbital degeneracy. At low temperature the structural distortion introduces an orbital anisotropy that is responsible for the static structure observed. Hence, a valence bond crystal state with fixed position of dimers is more appropriate for the low temperature phase, than a resonating valence bond configuration.

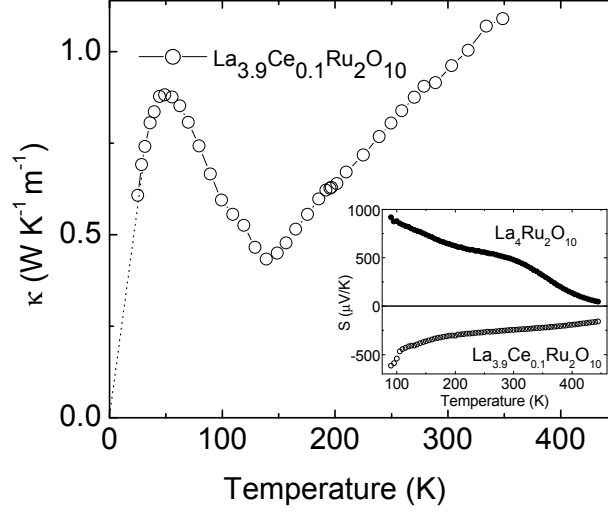


Figure 6. Temperature dependence of the thermal conductivity in $\text{La}_{3.9}\text{Ce}_{0.1}\text{Ru}_2\text{O}_{10}$. Inset: Thermoelectric power for the pure and Ce-doped sample. The hole-to-electron conduction after Ce-doping demonstrates the effective electron doping.

In this situation, the scenario predicted by equation (1) is completely modified above T_S : the Umklapp process must be largely suppressed, and the assumptions under Rayleigh dispersion mechanism are no longer applicable. In fact, when the defect is comparable in size or larger than the phonon wavelength, Joshi¹⁹ obtained an inverse relaxation time which is dependent on ω^2 instead of ω^4 . Making use of this frequency dependence, we obtained the linear $\kappa(T)$, shown in Figure 4 ($n=2$, $C = 4.5 \times 10^8 \text{ s}$, $A=3.6 \times 10^9 \text{ s}^{-1}$, $B=0$, in equation (2)), that fits the experimental data nicely above T_S .

Another source of linear $\kappa(T > T_S)$ in crystalline materials is the existence of Raman scattering, due to optical-acoustic coupling.^{12,20} Although optical modes are not effective in transporting heat due to their small group velocity, they can interact with acoustic phonons under certain circumstances, influencing very much the heat transport. Dynamic disorder in systems with loosely bond guest species (clathrate, skutterudites) reduces the energy of high-frequency lying optical modes and flattens the phonon bands, reducing the velocity of the acoustic phonons and therefore the thermal conductivity.²¹ This mechanism introduces a dominant term in $\kappa \propto T$, which is qualitatively similar to the behavior of glasses and highly disordered systems like clathrate hydrates²² and polymers,²⁰ and reproduces the temperature dependence we observed in the HT phase in $\text{La}_4\text{Ru}_2\text{O}_{10}$.

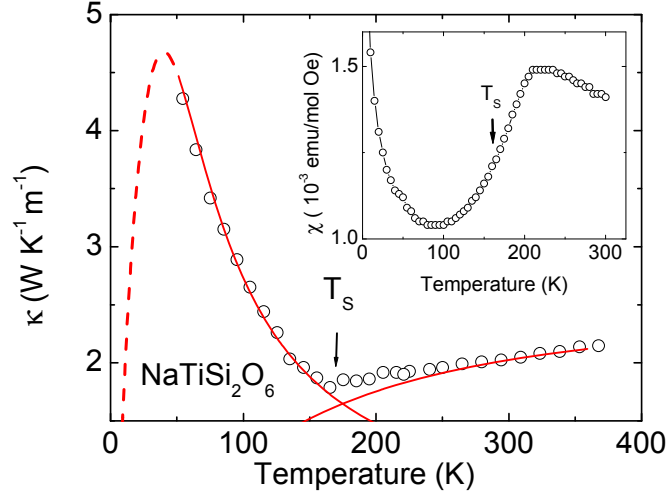


Figure 7. Temperature dependence of thermal conductivity for $\text{NaTiSi}_2\text{O}_6$. The vertical arrow marks the transition to the low temperature spin-singlet phase. Due to the large thermal conductivity at low temperatures, we were unable to extend the measurements down to lower temperatures in our experimental setup. Solid lines represent the fittings according to equation (1), see text for details. The dotted line is an extension to low temperature of the fitting below T_s . Inset: Temperature dependence of the magnetization at $H=1\text{ T}$. The transition temperature, T_s , is defined from the maximum in the derivative of the $M(T)$ curve.

The distribution of phonons tends to be concentrated around a particular energy at a given temperature, approximately equal to $\approx 1.6k_B T$.¹³ For a $\Theta \approx 225\text{ K}$, this corresponds to maximum phonon energy of $\approx 30\text{ meV}$. Wu *et al.*²³ observed drastic changes in the optical phonon modes between ≈ 12 to 75 meV , showing that this optical-acoustic interaction is indeed a realistic possibility. At the light of our data, a complete description of the phonon spectrum of $\text{La}_4\text{Ru}_2\text{O}_{10}$ is highly desirable, for a quantitative fitting of $\kappa(T > T_s)$.

Finally, in order to test the generality of this effect in other systems with orbital-induced spin-pairing, we have measured the thermal conductivity in $\text{NaTiSi}_2\text{O}_6$.²⁴ The magnetic susceptibility of this material decreases sharply below $\approx 200\text{ K}$ (see Figure 7, inset), indicating the transition to a non-magnetic singlet state with alternating short-long Ti-Ti bond distances. The magnetostructural transition is accompanied by an orbital ordering, that introduces the necessary exchange anisotropy for the spin dimerization. Above the transition, Konstantinovic *et al.*²⁵ observed an anomalous broadening of several phonon modes in the Raman spectra, that could be compatible with bond-length fluctuations.

The results of the thermal conductivity for $\text{NaTiSi}_2\text{O}_6$ and the fitting to the Debye model are shown in Figure 7. To fit the low temperature part ($T < T_s$) the relaxation time due to boundary scattering, $A = 1.0 \times 10^9\text{ s}^{-1}$, was calculated directly from experimental parameters ($\Theta \approx 450\text{ K}$ from Ref. [24] and diameter $\approx 2.5\text{ }\mu\text{m}$). For Rayleigh dispersion we considered the existence of a 5% of defects in the propagation of the short-long Ti-Ti bonds, that produce a variation $\approx 7\%$ in the bond distance, to give a $C = 3(\pm 1).0 \times 10^{-42}\text{ s}^3$. The latter parameter is considerably smaller than in the case of the $\text{La}_4\text{Ru}_2\text{O}_{10}$, due to

larger sound velocity in $\text{NaTiSi}_2\text{O}_6$. The Umklapp scattering factor calculated from the experimental parameters $B=1.25\times 10^{-18} \text{ s K}^{-1}$, ($\alpha=3$) which in this case is about ten times smaller than the best fitting factor $B=1.5\times 10^{-17} \text{ s K}^{-1}$.

Above T_s , $\kappa(T)$ shows the linear behavior characteristic of glasses compatible with the persistence of dynamic bond-length distortions due to fluctuating orbital occupancy. However, the increase is much slower than in $\text{La}_4\text{Ru}_2\text{O}_{10}$, and a correct fitting of the high temperature data in $\text{NaTiSi}_2\text{O}_6$ can be obtained adding the Joshi scattering term ($n=2$, $D=5.4\times 10^7 \text{ s}$ in equation (2)) to boundary and Umklapp terms defined for low temperature (the contribution from Rayleigh scattering is negligible above T_s).

Similar glass-like dependent thermal conductivity was reported in the orbitally disordered state of correlated perovskites (AMnO_3 , RVO_3 , etc), where semicovalent exchange striction introduces local bond-length fluctuations.²⁶

Following these ideas, reducing even further the Jahn-Teller stabilization energy playing with t_{2g} electrons of 4d ions, combined with S or Se anions, could be a good place to look for systems in which the orbital liquid state is kept down to zero kelvin.²⁷

Summarizing, the HT phase of $\text{La}_4\text{Ru}_2\text{O}_{10}$ is best described as a resonating mixture of different orbital orderings. This implies that orbital degrees of freedom are not quenched above the orbital-ordering transition, but remain in a state of rapid fluctuating occupancy. The same behavior is reported in the spin-gap compound $\text{NaTiSi}_2\text{O}_6$. Given the strong coupling among the orbital, lattice, spin and charge degrees of freedom that characterizes strongly correlated electron systems, liquid-like states in the spin and charge sectors are probable as well. Furthermore, this effect could be exploited to reduce the lattice thermal conductivity in correlated oxides, to foster their applicability in thermoelectric devices.

Acknowledgments. We acknowledge discussion with Prof. J. B. Goodenough, Prof. D. Khomskii, Dr. N. Perkins, Dr. J. Deisenhoffer, Dr. V. Pardo and Dr. I. Gonzalez. F. R. Acknowledges funding from ERC (Starting Grant 259082-2DTHERMS), Ministry of Science of Spain (MAT2010-16157), and Xunta de Galicia (INCITE09-209-101-PR). Facilities used by H.-D. Z. are supported in part by NSF through cooperative agreement No. DMR-0654118 and the State of Florida, USA.

¹ J. B. Goodenough, in *Magnetism and the Chemical Bond*, edited by John Willey and Sons, New York, 1963.

² D. I. Khomskii, Prog. Theor. Phys. Suppl. **159**, 319 (2005).

³ M. J. Konstantinovic, J. van den Brink, Z. V. Popovic, V. V. Moshchalkov, M. Isobe, Y. Ueda, Phys. Rev. B **69**, 020409 (2004).

⁴ H. Wu, Z. Hu, T. Burnus, J. D. Denlinger, P. G. Khalifah, D. G. Mandrus, L.-Y. Jang, H. H. Hsieh, A. Tanaka, K. S. Liang, J. W. Allen, R. J. Cava, D. I. Khomskii, L. H. Tjeng, Phys. Rev. Lett. **96**, 256402 (2006).

⁵ D. I. Khomskii, T. Mizokawa, Phys. Rev. Lett. **94**, 156402 (2005).

⁶ P. Khalifah, R. Osborn, Q. Huang, H. W. Zandbergen, R. Jin, Y. Liu, D. Mandrus, R. J. Cava, Science **297**, 2237 (2002).

⁷ R. Heary, D. Coffey, M. De Marco, P. Khalifah, S. Toorongian, M. Haka, Phys. B **393**, 78 (2007).

⁸ S. J. Moon, W. S. Choi, S. J. Kim, Y. S. Lee, P. G. Khalifah, D. Mandrus, T. W. Noh, Phys. Rev. Lett. **100**, 116404 (2008).

⁹ A. H. Carim, P. Dera, L. W. Finger, B. Mysen, C. T. Prewitt, D. G. J. Schlom, Solid State Chem. **149**, 137 (2000).

¹⁰ D. Bloch, J. Phys. Chem. Solids **27**, 881 (1965).

¹¹ W. A. Harrison, in *Electronic Structure and the Properties of Solids*, edited by W. H. Freeman and Company, San Francisco, 1980.

-
- ¹² *Thermal Conductivity. Theory, Properties and Applications*, edited by T.M. Tritt Kluwer Academic/Plenum Publishers, New York, 2004.
- ¹³ J. M. Ziman, in “*Electrons and Phonons*”, Int. Series of Monographs in Phys., Oxford Clarendon Press, Oxford, 1963.
- ¹⁴ G. A. Slack, S. Galginaitis, Phys. Rev. **113**, A253 (1964).
- ¹⁵ C. T. Walker, R. O. Pohl, Phys. Rev. **131**, 1433 (1963).
- ¹⁶ S.K. Malik, Darshan C. Kundaliya, R.D. Kale, Solid State Comm. **135**, 166 (2005).
- ¹⁷ C. Kittel, Phys. Rev. **75**, 972 (1949).
- ¹⁸ M. C. Sánchez, G. Subías, J. García, J. Blasco, Phys. Rev. Lett., **90**, 045503 (2003).
- ¹⁹ Y. P. Joshi, Phys. Stat. Sol. (b) **95**, 627 (1979).
- ²⁰ M. N. Wybourne, B. J. Kiff, D. N. Batchelder, Phys. Rev. Lett. **53**, 580 (1984).
- ²¹ M. Christensen, A. B. Abrahamsen, N. B. Christensen, F. Juranyi, N. H. Andersen, K. Lefmann, J. Andreasson, C. R. H. Bahl, B. B. Iversen, Nat. Mat. **7**, 811 (2008).
- ²² J. S. Tse, M. A. White, J. Phys. Chem. **92**, 5006 (1988).
- ²³ D. Wu, P. Khalifah, D. G. Mandrus, N. L. Wang, J. Phys.: Condens. Matter **20**, 325204 (2008)
- ²⁴ M. Isobe, E. Ninomiya, A. N. Vasilev, Y. Ueda, J. Phys. Soc. Jpn **71**, 1423 (2002).
- ²⁵ M. J. Konstantinovic, J. van den Brink, Z. V. Popovic, V. V. Moshchalkov, M. Isobe, Y. Ueda, Phys. Rev. B **69**, 020409 (2004).
- ²⁶ J.-Q. Yan, J.-S. Zhou, J. B. Goodenough Phys. Rev. Lett. **93**, 235901 (2004).
- ²⁷ G. Khaliullin, S. Maekawa, Phys. Rev. Lett. **85**, 3950 (2000).